

# Omni-Referring Image Segmentation

Qiancheng Zheng<sup>1\*</sup>, Yunhang Shen<sup>2\*</sup>, Gen Luo<sup>3</sup>, Baiyang Song<sup>1</sup>, Xing Sun<sup>2</sup>,  
Xiaoshuai Sun<sup>1</sup>, Yiyi Zhou<sup>1†</sup>, Rongrong Ji<sup>1</sup>

<sup>1</sup> Key Laboratory of Multimedia Trusted Perception and Efficient Computing,  
Ministry of Education of China, Xiamen University, 361005, P.R. China.

<sup>2</sup> YouTu Lab, Tencent, P.R. China. <sup>3</sup> OpenGVLab, Shanghai AI Laboratory.

{qianchengzheng, songbaiyang}@stu.xmu.edu.cn, {zhouyiyi, xssun, rrji}@xmu.edu.cn,  
luogen@pjlab.org.cn, shenyunhang01@gmail.com

## Abstract

In this paper, we propose a novel task termed Omni-Referring Image Segmentation (OmniRIS) towards highly generalized image segmentation. Compared with existing unimodally conditioned segmentation tasks, such as RIS and visual RIS, OmniRIS supports the input of text instructions and reference images with masks, boxes or scribbles as omni-prompts. This property makes it can well exploit the intrinsic merits of both text and visual modalities, i.e., granular attribute referring and uncommon object grounding, respectively. Besides, OmniRIS can also handle various segmentation settings, such as one v.s. many and many v.s. many, further facilitating its practical use. To promote the research of OmniRIS, we also rigorously design and construct a large dataset termed OmniRef, which consists of 186,939 omni-prompts for 30,956 images, and establish a comprehensive evaluation system. Moreover, a strong and general baseline termed OmniSegNet is also proposed to tackle the key challenges of OmniRIS, such as omni-prompt encoding. The extensive experiments not only validate the capability of OmniSegNet in following omni-modal instructions, but also show the superiority of OmniRIS for highly generalized image segmentation. The code and dataset will be available at [link](#).

## 1. Introduction

Recent years have witnessed the great advancement of image segmentation moving from the traditional fixed-category masking to the open-ended ones conditioned on text or visual reference [15, 16, 22, 45, 46]. For instance, the popular Referring Image Segmentation (RIS) [12], also known as Referring Expression Segmentation (RES) [33],

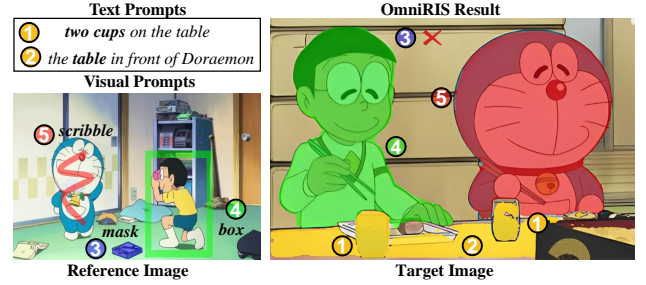


Figure 1. Illustration of the proposed Omni-Referring Image Segmentation (OmniRIS) task. OmniRIS can support text expressions (1,2) and reference images with mask (3), box (4) or scribble (5) prompts under the settings of one v.s. one, one v.s. many, many v.s. many or no-target.

can segment the referents of arbitrary types in an image according to the given text description, exhibiting much better flexibility than traditional segmentation tasks [9, 39]. Recent RIS tasks, e.g., Generalized Referring Expression Segmentation (GRES) [26], further extend the segmentation patterns to multi-target or no-target grounding. More recently, practitioners also resort to visual reference for the identification of similar visual objects in images [22, 30, 53, 59], which we term Visual RIS here.

Despite their great successes, existing referring segmentation tasks still have their own shortcomings due to the inherent properties of the unimodal prompts they use. In particular, the text expressions used for RIS can help the model locate common objects with specific attributes or spatial relationships in a rich image. For instance, finding “two cups on the table” as shown in Fig. 1. However, for the referents that are difficult to describe, RIS models often suffer from low precision [33, 55]. In contrast, Visual RIS can well mitigate this issue by referring to a reference image of the target object, also shown in Fig. 1. But in order to maintain a high recall rate, existing visual RIS methods [45, 46] are hard to identify objects of the same category but with dif-

\*Equal Contribution

†Corresponding Author

ferent details. In this context, it is natural to question that: “Is it plausible to combine the merits of both text and visual references to form a more effective segmentation manner?”

To approach this target, we propose a novel task termed *Omni-Referring Image Segmentation* (OmniRIS) in this paper, of which illustration is given in Fig. 1. As discussed above, OmniRIS can support the inputs of text instructions or reference images, or both, to fully exploit the advantages of the two modalities, *i.e.*, *granular attribute referring* and *uncommon object grounding*, respectively. To correctly identify the referred visual semantics, OmniRIS also requires the model to be aware of masks, boxes or scribbles as additional prompts, which can also facilitate its practical use in terms of human-computer interaction. For a broader scope of application, OmniRIS also supports multiple forms of referring segmentation like GRES [26, 51], *i.e.*, the referring segmentation of *one v.s. many* or *no-target*, while the settings of *many v.s. many* and *many v.s. one* are first introduced to the RIS task. Moreover, OmniRIS also allows the switch between uni- and omni-modal prompts for better generalization. Overall, these properties help OmniRIS to achieve highly generalized image segmentation.

Despite these apparent merits, OmniRIS also has its intrinsic challenges. In addition to multimodal reasoning, a shared problem with previous RIS tasks [16, 22, 62], OmniRIS first encounters the issue of how to jointly model the prompts of text and visual modalities. Specifically, a decent OmniRIS model should be capable of learning text expressions and the reference images with spatial prompts at the same time. During inference, the multimodal embedding space it constructs should also allow for the grounding with unimodal or multimodal prompts, posing a key challenge for the multimodal designs of OmniRIS. Moreover, the training of an OmniRIS model is also intractable due to the flexible but complex task settings. As discussed above, OmniRIS also needs to handle five cases of segmentation which may involve potential referring conflicts, *e.g.*, *many v.s. many*. When given the text and visual prompts simultaneously, the referred objects are often distinct due to the different prompt content. Meanwhile, its other settings, such as *one v.s. one* and *no-target*, also need to be considered. Overall, OmniRIS is a novel but challenging task with great potential for highly interactive segmentation applications.

To facilitate the research of OmniRIS, we first propose a large dataset in this paper, termed *OmniRef*. OmniRef consists of 186,939 omni-prompts for 30,956 images. Among them, 78,585 prompts for 6,549 images are reserved for three test splits, *i.e.*, the *text-only*, *visual-only* and *omni* ones. As shown in Fig. 2, its scale has surpassed that of existing popular RIS benchmarks, such as RefCOCO+/g [19, 35, 56] and gRefCOCO [26]. The OmniRef dataset is constructed in a rigorous way, which has strict criteria for the selection of images and the annotation

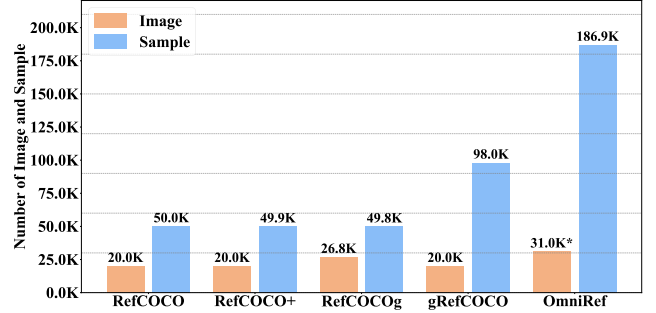


Figure 2. Statistical comparison between our OmniRef dataset and existing popular RIS datasets. \*The reference images (26,859) of OmniRef are not counted.

of omni-prompts, as shown in Fig. 5. Based on OmniRef, we also propose a strong baseline model called *OmniSegNet*, which is equipped with a novel *omni-prompt encoder* to handle the issue of omni-prompt modeling and a training regime to tackle the complex settings of OmniRIS.

Based on the proposed OmniRef dataset, we extensively examine the proposed OmniSegNet on the three test splits, and also compare it with a set of advanced uni-modal RIS methods [14, 21, 26, 51], of which results show its merits in handling unimodal and omni-modal prompts. Moreover, a bunch of qualitative analyses are also conducted to demonstrate the superiority of OmniRIS towards highly generalized image segmentation. For instance, the well trained OmniSegNet can be well generalized one-shot segmentation tasks with unseen reference images, as shown in Fig. 7.

In summary, our contributions are three-fold:

- We propose a novel task towards highly generalized image segmentation, termed *Omni-Referring Image Segmentation* (OmniRIS), which supports the inputs of text and visual instructions with omni-prompts.
- We construct a large dataset to facilitate the research of OmniRIS, termed *OmniRef*, which contains 186,939 omni-modal prompts for 30,956 images.
- We propose a strong baseline model *OmniSegNet*, which adopts a novel omni-prompt encoder and a carefully designed training regime to overcome the key challenges of OmniRIS.

## 2. Related Works

### 2.1. Referring Image Segmentation

*Referring Image Segmentation* (RIS) denotes the segmentation of target instances in an image according to the given reference information [1, 27, 54, 58]. In existing literature, RIS mainly refers to the use of text descriptions as the task prompt, *i.e.*, *Referring Expression Segmentation* (RES) [26, 29, 34, 48] or *visual grounding* [3, 17, 28, 44, 52, 61]. Early RIS methods [12, 33] often consider RIS as a text-mask matching problem, and adopt a multi-step pipeline

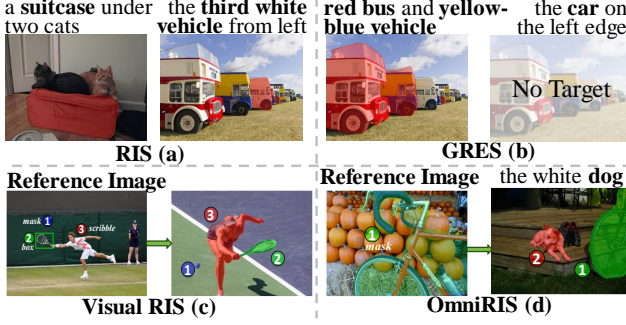


Figure 3. Comparison between OmniRIS and existing unimodal referring segmentation tasks. RIS (a) segments the visual referent corresponding to the given text expression, based on which GRES (b) extends its types of outputs, such as *one* v.s. *many* and *no-target*. Visual RIS (c) refers to the grounding based on the referenced instances in another image. Compared with existing RIS tasks, the proposed OmniRIS (d) merges the merits of text and visual information to support more flexible image segmentation.

with additional relationship feature learning [24, 42, 57]. Subsequent research reformulates this task as an end-to-end and cross-modal mask regression problem, and adopts one-stage attention-based models for the joint modeling of multi-modal fusion and reasoning [5, 27, 50]. Recently, a set of works [13, 26, 51] have been proposed to extend the segmentation settings of RIS. For instance, Liu *et al.* [26] propose the GRES benchmark to extend RIS to more settings, such as *one* vs. *many* and *no-target* cases. GSVA [51] leverages large multimodal models to better handle diverse referring expressions in GRES. However, these advancements only focus on text-conditioned RIS.

## 2.2. Visually Referring Image Segmentation

*Visually Referring Image Segmentation* (Visual RIS) aims to segment objects in a target image based on visual references [11, 30, 46, 59]. In practice, visual references can be conveyed through various prompt types, such as masks, boxes, or scribbles, and have been widely adopted in one-shot or few-shot segmentation frameworks [10, 36, 38, 47, 60]. For example, VRP-SAM [45] enhances SAM [20] by introducing visual reference prompts to improve performance in complex scenes. Despite the progress, many existing methods rely on predefined prompt formats and mainly focus on single-image settings, limiting the flexibility and cross-image generalization. Furthermore, mainstream visual prompting techniques [16, 22, 23, 62] are inferior in capturing consistent cross-image semantics. This shortcoming hinders the alignment and fusion of reference and target features, restricting the effectiveness of Visual RIS in real-world applications. Compared with text-based RIS, visual RIS is less ambiguous and provides explicit object appearances, but it requires extra reference images or masks and lacks the descriptive flexibility of attribute referring. Over-

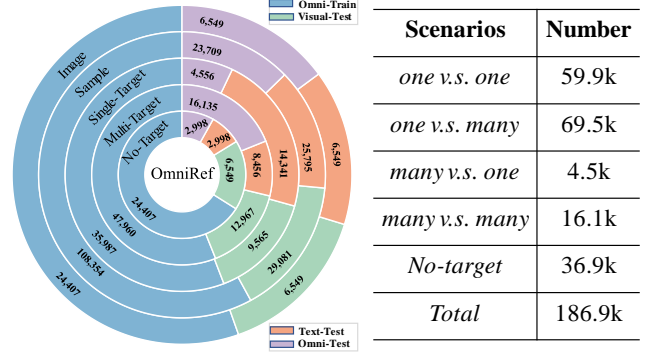


Figure 4. Statistics of the training set and three test splits of OmniRef. Those splits all involve the segmentation outputs of single-target, multi-target and no-target, as well as the cases of *one* v.s. *one*, *one* v.s. *many*, *many* v.s. *one*, *many* v.s. *many* and *no-target*.

all, omni-modal prompts that aim to unify text and visual prompts have not been effectively handled yet.

## 3. The Definition of OmniRIS

In this paper, we propose a novel task for highly generalized image segmentation, termed *omni-referring image segmentation* (OmniRIS). As shown in Fig. 1 and Fig. 3, OmniRIS takes text instructions, reference images or both as input, and it also supports different spatial prompts to specify the referents in images, such as masks, boxes or scribbles.

Concretely, given a target image  $I_t \in \mathbb{R}^{H \times W \times 3}$ , OmniRIS supports a set of multimodal prompts  $\mathcal{P}$ , defined by

$$\mathcal{P} = \{T, (I_r, P_s)\}, \quad (1)$$

where  $T$  is a text instruction and  $I_r \in \mathbb{R}^{H \times W \times 3}$  is a reference image.  $P_s$  denotes the spatial prompts, all represented as binary matrices  $P_s \in \mathbb{R}^{H \times W}$  of the same size as the reference image. These include the segmentation masks  $P_{\text{mask}}$ , boxes  $P_{\text{box}}$  and scribbles  $P_{\text{scribble}}$ . Note that each element in  $\mathcal{P}$  is optional, enabling the flexible omni-modal interaction. Thus, the objective of OmniRIS is defined by

$$f_\theta : (I_t, \mathcal{P}) \rightarrow (\{M_k\}_{k=1}^K, y). \quad (2)$$

where  $f_\theta$  is a parameterized model. The output consists of  $K$  binary segmentation masks  $M_k \in \{0, 1\}^{H \times W}$ , each corresponding to the objects referred to by the specific prompt in  $\mathcal{P}$ , and a binary indicator  $y \in \{0, 1\}$  for the existence of the referred objects in the target image. The number of predicted masks  $K$  is adaptively determined based on the number of input prompts.

From the above definitions, we can see that OmniRIS forms a highly flexible and generalized segmentation manner. In practice, we can use either text or reference images, or both, to mask the referents in the given image. The comparison to existing RIS tasks is illustrated in Fig. 3.



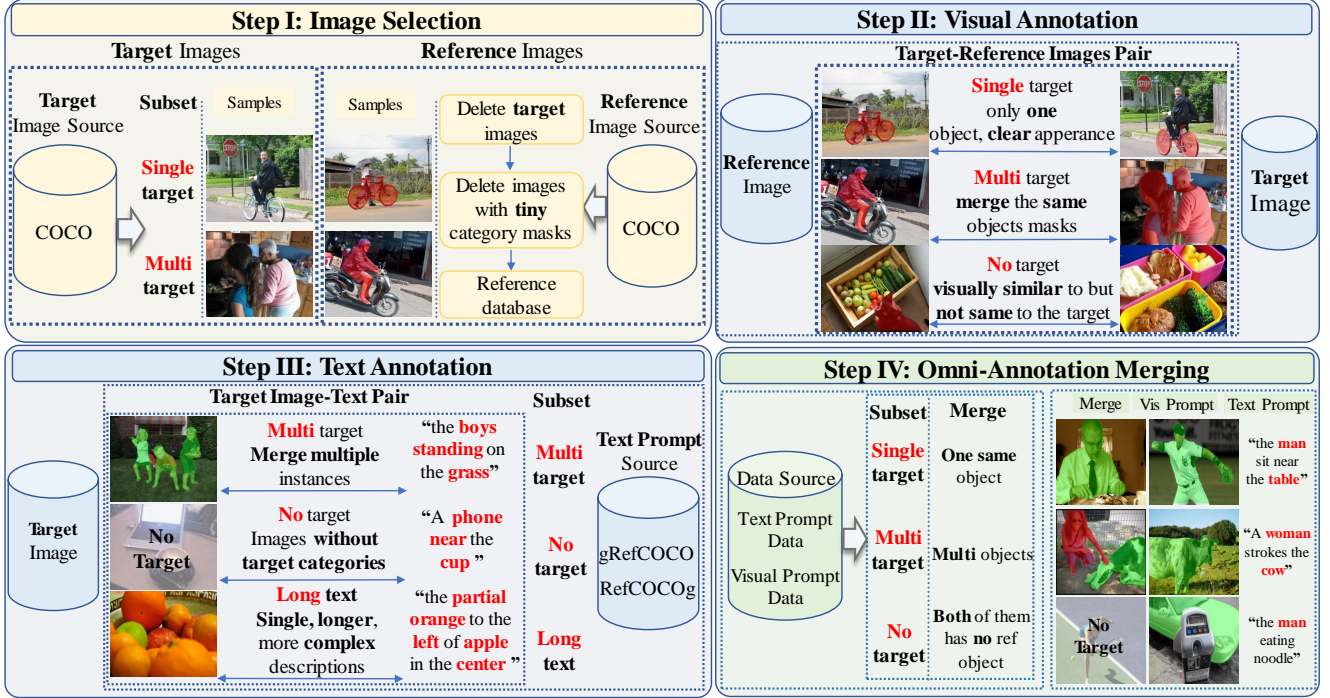


Figure 5. The construction pipeline of the proposed OmniRef dataset, which consists of four main steps. Step I filters out the images that have too few objects and lack visual diversity, and selects the ones containing multiple categories and spatially well-distributed objects as the target and reference images. Step II pairs the target and reference images to construct visual prompts for different segmentation cases. Step III aligns text prompts with target images that involve diverse cases, including the *single-target*, *multi-target* and *no-target* outputs with long and complex expressions. Step IV merges visual and text annotations to form the final omni-modal examples. After the four steps, manual checking is also conducted to ensure the quality of examples.

**Main Challenges.** Despite the obvious merits in flexibility, OmniRIS is also more challenging than previous RIS tasks. Above all, OmniRIS needs to cope with the prompts of more modalities than previous tasks. And how to help the OmniRIS model be capable of all types of prompts is the first challenge. Moreover, the various segmentation settings also pose more obstacles to the modeling and training of OmniRIS, *e.g.*, enabling the use of single and omni-modal prompts in one model and handling the cases of single-target, multi-target and no-target at the same time. Overall, these properties make OmniRIS a challenging task but one with great potential in various segmentation applications.

## 4. OmniRef: A Large OmniRIS Dataset

To facilitate the research of OmniRIS, we propose a large dataset in this paper, termed *OmniRef*. OmniRef has 186,939 samples from a total of 30,956 images and the corresponding annotations, such as masks, boxes and scribbles. The detailed statistics of OmniRef are reported in Fig. 4.

### 4.1. Dataset Composition

OmniRef has 30,956 images with 186,939 omni-prompts. Besides, it also has a high-quality visual reference set consisting of 26,859 images with 34,570 instances for visual

prompting. These data are divided into the training and three test splits. In terms of the training set, *i.e.*, *Omni-Train*, it has 24,407 images and 108,354 prompts in total, which includes three types of segmentation outputs, namely *single-target* (35,987), *multi-target* (47,960) and *no-target* (24,407) ones. For the omni-prompts, it has 23,709 test prompts and 6,549 reference images, where the latter all include the spatial prompts of masks, boxes and scribbles. In terms of testing, OmniRIS considers the evaluations of both unimodal and omnimodal RIS. Thus, we build three test splits, namely *Text-test*, *Visual-test* and *Omni-test* splits. These three test sets share a total of 6,549 images. The text-test split has 25,795 text prompts, while the visual-test one has 29,081 visual prompts. The omni-test split further merges the data of the unimodal ones, including 23,709 omni-prompts. These three test splits are also collected with a balanced distribution of single-target, multi-target and no-target outputs, facilitating the comprehensive evaluation across different application scenarios.

### 4.2. Dataset Construction

To build the OmniRef dataset, we design a rigorous four-step pipeline to ensure the quality and correctness of its examples of which process is depicted in Fig. 5.

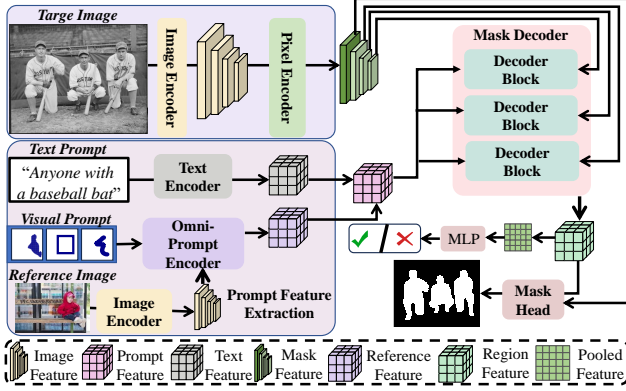


Figure 6. The architecture of the proposed OmniSegNet. OmniSegNet introduces a novel omni-prompt encoder to handle the spatial prompts, such as mask, box and scribble. With this omni-prompt encoder, the semantics of the visual referent in the image can be extracted to guide mask decoding. OmniSegNet can also support the processing of visual and text prompts at the same time.

**Step I: Image Selection.** We first select high-quality images from the popular MSCOCO dataset [25], similar to previous RIS benchmarks [19, 26, 56]. The selection criterion is that the image content should be rich and diverse enough, thereby providing sufficient semantic context for constructing OmniRIS. To achieve this, we filter out images that contain too few object instances and retain those containing multiple categories and spatially well-distributed objects, ensuring visual complexity. Lastly, we obtain a total of 30,956 images for the OmniRef dataset.

**Step II: Visual Annotation.** Next, we build the visual reference set with masks, boxes and scribbles as the omni-prompts. Following the previous step, we first collect 26,859 images from the remaining ones of MSCOCO, and these images all contain obvious visual instances. For these reference images and their visual instances, we then obtain the object masks directly from the instance-level annotations of MSCOCO, ensuring both accuracy and consistency. Based on these masks, we further use the scripts to generate corresponding box and scribble prompts. Specifically, boxes are created by computing the tight bounding rectangles around the mask regions, while scribbles are generated by randomly drawing lines or dots within the mask area. Via this procedure, we create the visual reference set consisting of 34,570 visual prompt samples.

Lastly, we conduct the annotation of these visual prompts to OmniRef’s images. For each target image in OmniRef, we select reference images whose categories match those in the target images, and then form the positive pairs under *multi-target* and *single-target* settings. In the *multi-target* case, the instances of the same category in the target image are merged into one mask, which is then paired with a corresponding reference mask. In the *single-target* case, only one instance is retained. For the *no-target* case,

reference images are paired with the target images one by one. These reference images are visually similar to the corresponding targets but contain categories absent from them, serving as challenging negative pairs.

**Step III: Text Annotation.** After the visual annotation, we collect the text prompts for OmniRef’s images. Specifically, we reorganize text prompt samples from the validation and test splits of gRefCOCO [26] and RefCOCOg [19] based on the target count and instruction complexity. Multi-target samples are collected from gRefCOCO by identifying images with text prompts pointing to different object instances. For no-target samples, we extract text prompts whose referred objects are absent in the image. To enrich the diversity of expression content, we use RefCOCOg to support long-text and single-target evaluation, retaining those samples that refer to a single object using more complex or lengthy descriptions. Finally, each image in OmniRef is associated with multiple text prompts.

**Step IV: Omni-Annotation Merging.** After the text annotation, we finally merge the omni-modal prompts for OmniRef’s images. We combine the visual and text prompts obtained in the previous two steps that refer to the same target image, thereby constructing omni-modal referring data. Specifically, for *multi-target* cases, the two prompts are required to refer to different object categories within the image. If they refer to the same category, the prompts must jointly cover all its instances. For *single-target* cases, both prompts refer to the same object instance, and the instance must be the only one of its category in the image. For *no-target* cases, the referred objects must not appear in the target image. Lastly, each image in the OmniRef evaluation set is paired with both visual and text prompts.

### 4.3. Evaluation Protocols

In terms of evaluation, OmniRIS includes the metrics of *No-Target Accuracy* ( $N_{acc}$ ) [26], *Cumulative IoU* (cIoU), *Generalized IoU* (gIoU), and  $Pr@X$  for comprehensive assessment.  $N_{acc}$  measures the performance of no-target samples, cIoU is the *intersection-over-union* ratio, and gIoU averages IoU across all samples. For no-target, true positives/negatives are assigned IoUs of 1/0.  $Pr@X$  denotes the percentage of samples whose IoU exceeds a threshold  $X$ , where no-target samples are excluded. For multi/single-target samples, the threshold is set to 0.7 due to their larger foreground regions.

## 5. The Baseline Model

In this paper, we also propose a strong and general baseline model for OmniRIS, termed *OmniSegNet*, of which the structure is illustrated in Fig. 6.

Concretely, given a target image  $I_t$ , OmniSegNet first extracts its features  $F_v$  by the vision backbone, and then

Table 1. Comparison between OmniSegNet and existing text and visual RIS methods on three test splits of OmniRef. OmniSegNet exhibits strong and generalized capabilities of both unimodal and omnimodal referring segmentation.

Methods	Backbone	Text Encoder	Text-test			Visual-test			Omni-test		
			cIoU	gIoU	N <sub>acc</sub>	cIoU	gIoU	N <sub>acc</sub>	cIoU	gIoU	N <sub>acc</sub>
MLLM Methods											
LISA-7B [21]	ViT-H	Vicuna-7B	64.95	66.02	-	-	-	-	-	-	-
GSVA-7B [51]	ViT-H	Vicuna-7B	65.30	67.57	63.44	-	-	-	-	-	-
Specialist Methods											
DIT [14]	ViT-B	BERT	60.72	62.73	-	-	-	-	-	-	-
ReLA [26]	Swin-B	BERT	63.40	64.75	57.97	-	-	-	-	-	-
GF-SAM [59]	ViT-L	-	-	-	-	40.66	42.46	-	-	-	-
Matcher [30]	ViT-L	-	-	-	-	41.29	42.04	-	-	-	-
VRP-SAM [45]	ViT-L	-	-	-	-	55.70	52.74	78.63	-	-	-
DCAMA [43]	Swin-B	-	-	-	-	60.23	49.91	80.46	-	-	-
VRP-SAM+ReLA	ViT-L	BERT	<u>63.40</u>	<u>64.75</u>	<u>57.97</u>	55.70	<u>52.74</u>	78.63	61.32	<u>59.07</u>	55.71
DCAMA+ReLA	Swin-B	BERT	<u>63.40</u>	<u>64.75</u>	<u>57.97</u>	<u>60.23</u>	49.91	<u>80.46</u>	<u>62.61</u>	58.08	<u>55.93</u>
OmniSegNet	Swin-B	BERT	<b>64.92</b>	<b>66.44</b>	<b>62.56</b>	<b>76.63</b>	<b>68.87</b>	<b>90.81</b>	<b>69.27</b>	<b>67.80</b>	<b>57.69</b>

enhances them via a PixelEncoder:

$$\mathbf{F}_m^0, \mathbf{F}_m^i = \text{PixelEncoder}(\mathbf{F}_v). \quad (3)$$

$\mathbf{F}_m^i$ , where  $i \in 1, 2, 3$ , is used for MaskDecoder, and  $\mathbf{F}_m^0$  is for the final mask prediction via MaskHead.

In terms of text prompts, text features  $\mathbf{F}_t$  are extracted by TextEncoder and directly fed to MaskDecoder. For reference images, they are first processed by the vision backbone to obtain the visual features  $\mathbf{F}_r$ . Afterwards, the visual features and the different spatial prompts are jointly modeled by the proposed *Omni-Prompt Encoder* consisting of a *Prompt Embed Module* (PEM) and the *Prompt Generator*:

$$\mathbf{F}_p = \text{PromptGenerator}(\text{PEM}(\mathbf{F}_r, \mathbf{P}), \mathbf{F}_q). \quad (4)$$

Here,  $\mathbf{P}$  denotes the spatial prompt from the reference image,  $\mathbf{F}_{vs}$  is the fused visual reference features,  $\mathbf{F}_q$  are learnable queries and  $\mathbf{F}_p$  is the final prompt embedding used to guide segmentation.

Lastly,  $\mathbf{F}_t$  and  $\mathbf{F}_p$  are combined and fed to MaskDecoder, as shown in Fig. 6. Due to the page limit, the details of our OmniSegNet are given in our **Appendix**.

**Training Regimes.** To tackle the complex settings of OmniRIS, we further introduce a three-step training regime for our OmniSegNet. *i. Vision-Language Alignment.* We first conduct the VL pretraining using the text RIS dataset, which aims to help OmniSegNet be capable of both instruction understanding and conditional segmentation. *ii. Visual Instruction Tuning.* Afterwards, we fix the text encoder and learn to project the visual prompt features onto the semantics of OmniSegNet using the visual prompt data of OmniRef. Via this process, OmniSegNet learns to be aware of visual conditions for segmentation. *iii. Joint Omni-modal*

Table 2. Ablation study of OmniSegNet on the Visual-test of the OmniRef. (a) shows the results of using different visual prompts. (b) ablates the settings of the prompt embed module.

Configuration	cIoU	gIoU	Pr@0.7	Pr@0.8	Pr@0.9
(a) Types of Visual Prompts					
<i>scribble</i>	73.20	63.31	47.17	35.85	15.08
<i>box</i>	74.00	64.21	48.84	36.71	14.99
<i>mask</i>	<b>75.35</b>	<b>66.36</b>	<b>52.68</b>	<b>40.61</b>	<b>18.30</b>
(b) Prompt Embed Module Fusion Methods					
-	62.61	55.63	40.36	30.10	11.77
<i>multiply</i>	74.61	64.31	49.39	37.52	16.27
<i>add</i>	<b>75.35</b>	<b>66.36</b>	<b>52.68</b>	<b>40.61</b>	<b>18.30</b>

*Training.* After the second step, OmniSegNet has been capable of both visual and text referring, but with degradations in text referring. Thus, we mix the omni-data for the joint training of OmniSegNet. The details can refer to our code project given in the supplementary materials.

## 6. Experiments

### 6.1. Quantitative Analysis

We first evaluate the set of visual and textual RIS methods as well as our OmniSegNet on the proposed OmniRef benchmark. Since existing RIS methods can only perform unimodal RIS tests, we also introduce two strong OmniRIS baselines in Tab. 1, *i.e.*, ReLA+VRP-SAM and ReLA+DCAMA. In these two baselines, ReLA is in charge of text examples of OmniRef, while VRP-SAM and DCAMA are used to process visual RIS examples. In terms of the text prompt evaluations, *i.e.*, *Text-test*, the MLLM-based method GSVA-7B [51] achieves the best performance on this test split, but it adopts much larger backbones than

Table 3. Evaluation of OmniSegNet on common RIS benchmarks. OmniSegNet achieves competitive performance under the Text-RIS evaluations, showing general performance for Text-RIS tasks.

Methods	Backbone	gRefCOCO			RefCOCO			RefCOCO+			RefCOCOg	
		val	testA	testB	val	testA	testB	val	testA	testB	val-u	test-u
MLLM Methods												
PixelLM-7B [40]	CLIP-ViT-L	-	-	-	73.00	76.50	68.20	66.30	71.70	58.30	69.30	70.50
LISA-7B [21]	ViT-H	61.76	68.50	60.63	74.90	79.10	72.30	65.10	70.80	58.10	67.90	70.60
GSVA-7B [51]	ViT-H	63.29	69.93	60.47	77.20	78.90	73.50	65.90	69.60	59.80	72.70	73.30
Specialist Methods												
DIT [14]	ViT-B	-	-	-	71.98	74.51	68.77	59.97	65.52	51.72	60.18	61.15
LAVT [55]	Swin-B	57.64	65.32	55.04	72.73	75.82	68.79	62.14	68.38	55.10	61.24	62.09
ReLA [26]	Swin-B	62.42	<u>69.26</u>	<u>59.88</u>	73.82	76.48	70.18	<b>66.04</b>	71.02	<u>57.65</u>	<b>65.00</b>	65.97
LQMFormer [41]	Swin-B	<u>64.98</u>	-	-	<b>74.16</b>	<u>76.82</u>	<b>71.04</b>	65.91	<b>71.84</b>	57.59	64.73	<u>66.04</u>
OmniSegNet	Swin-B	<b>65.30</b>	<b>70.98</b>	<b>62.18</b>	<u>74.02</u>	<b>76.93</b>	<u>70.63</u>	<u>65.95</u>	<u>71.30</u>	<b>58.31</b>	<u>64.90</u>	<b>66.27</b>

Table 4. One-shot Semantic Segmentation results (mIoU) on PASCAL-5<sup>i</sup> and LVIS-92<sup>i</sup> datasets.

Methods	PASCAL-5 <sup>i</sup>					LVIS-92 <sup>i</sup>
	5 <sup>0</sup>	5 <sup>1</sup>	5 <sup>2</sup>	5 <sup>3</sup>	Mean	Mean
PerSAM [60]	-	-	-	-	43.1	11.5
PerSAM-F [60]	-	-	-	-	48.5	<b>12.3</b>
Painter [49]	-	-	-	-	-	10.5
MIAPnet [37]	45.9	46.9	47.2	41.5	45.4	-
OmniSegNet	<b>56.0</b>	<b>52.9</b>	<b>53.8</b>	<b>49.3</b>	<b>53.0</b>	9.2

the other methods, *i.e.*, ViT-H [6] and the 7B-level LLM called Vicuna [2]. For the methods using the same-scale backbones, we can see that OmniSegNet can achieve better performance on this evaluation, showing its great capability in following text instructions. In the second block of Tab. 1, we compare OmniSegNet with four advanced visual RIS methods on the visual-test split. Since these methods cannot identify the existence of objects, we add a classification head to VRP-SAM and DCAMA and re-train them on OmniRef. Compared with these advanced visual RIS methods, our OmniSegNet also shows better performance on all three metrics, indicating its superiority in handling visual prompts. For the Omni-test, OmniSegNet surpasses the combined baselines ReLA+VRP-SAM and ReLA+DCAMA by a large margin, demonstrating its strong capability to seamlessly model and reason over both textual and visual modalities. Overall, these demonstrate the effectiveness and generalization of OmniSegNet.

### 6.1.1. Ablation Study of OmniSegNet

To understand the key components and design choices of OmniSegNet, we conduct ablation studies on three aspects: the types of visual prompts, the design of the *Prompt Embedding Module* (PEM) and the sampling ratio between text- and visual-guided data during training, whose detailed results are presented in the **Appendix**.

In Tab. 2 (a), we ablate the results of using different visual prompts. Specifically, *mask* provides the most comprehensive information about object features and effectively preserves the context of the reference object, so it performs best among all types of prompts. In contrast, *box* presents the suboptimal performance, mainly due to the noises contained in its box backgrounds. Similarly, *scribble* cannot fully capture the features of the object due to its irregular shape and limited coverage, resulting in the lowest performance. These observations indicate that the quality and completeness of visual prompts are important for OmniRIS. In Tab. 2 (b), we examine different fusion designs of the *Prompt Embedding Module* (PEM). Three settings are compared, which are *no fusion* (-), *multiplication-based fusion* (multiply) and *addition-based fusion* (add). When no fusion is applied, *i.e.*, the PEM is absent, there is no interaction between the reference visual features and the prompt embedding features. As a result, the model fails to accurately capture the characteristics of the target object. This implies the importance of the PEM in guiding the visual referring segmentation process. Furthermore, the method used to fuse prompt and reference features also affects performance. Compared to multiplication, the addition operation yields better results across all metrics. This can be attributed to the fact that addition provides a more stable and flexible feature integration, while multiplication may lead to information suppression.

### 6.1.2. Generalization of OmniSegNet

To validate the generalization of the proposed OmniSegNet, we also evaluate it on existing RIS benchmarks in Tab. 3. As shown in Tab. 3, on gRefCOCO, OmniSegNet surpasses the previous SOTA method ReLA with absolute gains of 2.88%, 1.72% and 2.30% on the three evaluation sets, respectively. Notably, it even outperforms the powerful MLLM-based methods such as LISA-7B [21] and GSA-7B [51] with absolute improvements of 2.01%, 1.05% and





Figure 7. Visualized predictions of OmniSegNet. The first block (Exp.1-9) shows text-only, visual-only and omnimodal samples from the OmniRef dataset, reflecting diverse scenarios such as *one* v.s. *one* (Exp.2), *one* v.s. *many* (Exp.1-2,4), *many* v.s. *one* (Exp.7), *many* v.s. *many* (Exp.6,8) and *no-target* (Exp.5,9). The last block (Exp.10-17) demonstrates the one-shot capability of OmniSegNet in handling unseen visual instances.

1.55% on the splits of gRefCOCO, respectively. In addition, OmniSegNet performs well on RefCOCO+/g, providing results comparable to the SOTA methods. On RefCOCO and RefCOCO+, the performance of our model is comparable to the MLLM-based methods such as LISA-7B [21] and PixelLM-7B [40]. Experimental results show that OmniSegNet performs strongly in text referring segmentation, achieving state-of-the-art results among specialist methods and delivering comparable or even superior accuracy to MLLM-based approaches.

To further examine the visual RIS capability, we also test OmniSegNet on One-shot Semantic Segmentation [37, 49, 60], even though this is not its primary design focus. To evaluate its potential in this task, we conduct experiments on the PASCAL-5<sup>i</sup> [7] and LVIS-92<sup>i</sup> [8] datasets. As shown in Tab. 4, OmniSegNet achieves competitive performance, particularly on PASCAL-5<sup>i</sup>, where it outperforms other comparison methods. Overall, these results well validate the generalization and designs of OmniSegNet.

## 6.2. Qualitative Analysis

To gain insights into the proposed OmniSegNet and OmniRIS task, we also visualize a set of predictions in Fig. 7. The experiments (Exp.1-17) reflect OmniSegNet’s capabilities across the diverse scenarios of the OmniRIS task, including *one* v.s. *one*, *one* v.s. *many*, *many* v.s. *one*, *many* v.s. *many* and *no-target* cases. For the text-only examples

(Exp.1-2), the model exhibits strong spatial reasoning and accurately grounds the referents based on complex instructions, such as “everyone on the left side of the scene” or “the knife on the bottom and the left carrot”, demonstrating its effectiveness in *one* v.s. *many* text-based segmentation. In the visual-only cases (Exp.3-5), OmniSegNet responds precisely to different types of visual prompts, including masks, boxes and scribbles. For example, given a reference image with a *box* indicating a *bear* (Exp.4), the model precisely segments the corresponding targets in the target image, highlighting its capability in *one* v.s. *one*, *one* v.s. *many* and *no-target* visual scenarios. Omnimodal examples (Exp.6-9) highlight OmniSegNet’s unique ability in processing omnimodal prompts by jointly leveraging textual and visual information, including *many* v.s. *one*, *many* v.s. *many* and *no-target* scenarios. Given the expression along with a corresponding reference image, the model produces semantically aligned and spatially accurate segmentation, showcasing its omnimodal fusion capability. Lastly, the examples in the last block (Exp.10-17) reflect OmniSegNet’s strong one-shot ability. When given unseen objects during testing, the model can still reliably locate and segment targets using only the provided prompts. These qualitative results confirm OmniSegNet’s comprehensive capabilities in the OmniRIS task and one-shot referring segmentation scenarios. Moreover, these examples highlight the merits of OmniRIS for highly generalized segmentation.



## 7. Conclusion

In this paper, we propose a novel task termed OmniRIS. Compared with existing unimodal RIS tasks, OmniRIS aims to merge the merits of both text and visual modalities to achieve highly generalized segmentation. In practice, OmniRIS can support the input of text descriptions and reference images with omni-prompts, such as masks, boxes and scribbles. Moreover, OmniRIS includes various segmentation settings, such as *many vs. many*. To support the research of OmniRIS, we also build a large dataset called OmniRef, based on which a strong and general baseline model called *OmniSegNet* is also proposed in this paper. Extensive experiments and analyses not only validate the advantages of OmniSegNet in handling both text and visual RIS tasks but also confirm the merits of OmniRIS towards highly generalized image segmentation.

## References

- [1] Silin Cheng, Yang Liu, Xinwei He, Sebastien Ourselin, Lei Tan, and Gen Luo. Weakmcn: Multi-task collaborative network for weakly supervised referring expression comprehension and segmentation. In *Proceedings of the Computer Vision and Pattern Recognition Conference*, pages 9175–9185, 2025. 2
- [2] Wei-Lin Chiang, Zhuohan Li, Ziqing Lin, Ying Sheng, Zhanghao Wu, Hao Zhang, Lianmin Zheng, Siyuan Zhuang, Yonghao Zhuang, Joseph E Gonzalez, et al. Vicuna: An open-source chatbot impressing gpt-4 with 90%\* chatgpt quality. See <https://vicuna.lmsys.org> (accessed 14 April 2023), 2(3):6, 2023. 7
- [3] Ming Dai, Lingfeng Yang, Yihao Xu, Zhenhua Feng, and Wankou Yang. Simvg: A simple framework for visual grounding with decoupled multi-modal fusion. *Advances in neural information processing systems*, 37:121670–121698, 2024. 2
- [4] Jacob Devlin. Bert: Pre-training of deep bidirectional transformers for language understanding. *arXiv preprint arXiv:1810.04805*, 2018. 13
- [5] Henghui Ding, Chang Liu, Suchen Wang, and Xudong Jiang. Vision-language transformer and query generation for referring segmentation. In *Proceedings of the IEEE/CVF international conference on computer vision*, pages 16321–16330, 2021. 3
- [6] Alexey Dosovitskiy, Lucas Beyer, Alexander Kolesnikov, Dirk Weissenborn, Xiaohua Zhai, Thomas Unterthiner, Mostafa Dehghani, Matthias Minderer, Georg Heigold, Sylvain Gelly, et al. An image is worth 16x16 words: Transformers for image recognition at scale. *arXiv preprint arXiv:2010.11929*, 2020. 7
- [7] Mark Everingham, Luc Van Gool, Christopher KI Williams, John Winn, and Andrew Zisserman. The pascal visual object classes (voc) challenge. *International journal of computer vision*, 88(2):303–338, 2010. 8
- [8] Agrim Gupta, Piotr Dollar, and Ross Girshick. Lvis: A dataset for large vocabulary instance segmentation. In *Proceedings of the IEEE/CVF conference on computer vision and pattern recognition*, pages 5356–5364, 2019. 8
- [9] Kaiming He, Georgia Gkioxari, Piotr Dollár, and Ross Girshick. Mask r-cnn. In *Proceedings of the IEEE international conference on computer vision*, pages 2961–2969, 2017. 1
- [10] Sunghwan Hong, Seokju Cho, Jisu Nam, Stephen Lin, and Seungryong Kim. Cost aggregation with 4d convolutional swin transformer for few-shot segmentation. In *European Conference on Computer Vision*, pages 108–126. Springer, 2022. 3
- [11] Mir Rayat Imtiaz Hossain, Mennatullah Siam, Leonid Sigal, and James J Little. Visual prompting for generalized few-shot segmentation: A multi-scale approach. In *Proceedings of the IEEE/CVF conference on computer vision and pattern recognition*, pages 23470–23480, 2024. 3
- [12] Ronghang Hu, Marcus Rohrbach, and Trevor Darrell. Segmentation from natural language expressions. In *Computer Vision—ECCV 2016: 14th European Conference, Amsterdam, The Netherlands, October 11–14, 2016, Proceedings, Part I 14*, pages 108–124. Springer, 2016. 1, 2
- [13] Yutao Hu, Qixiong Wang, Wenqi Shao, Enze Xie, Zhenguo Li, Jungong Han, and Ping Luo. Beyond one-to-one: Rethinking the referring image segmentation. In *Proceedings of the IEEE/CVF International Conference on Computer Vision*, pages 4067–4077, 2023. 3
- [14] Xiaorui Huang, Gen Luo, Chaoyang Zhu, Bo Tong, Yiyi Zhou, Xiaoshuai Sun, and Rongrong Ji. Deep instruction tuning for segment anything model. In *Proceedings of the 32nd ACM International Conference on Multimedia*, pages 905–914, 2024. 2, 6, 7
- [15] Menglin Jia, Luming Tang, Bor-Chun Chen, Claire Cardie, Serge Belongie, Bharath Hariharan, and Ser-Nam Lim. Visual prompt tuning. In *European conference on computer vision*, pages 709–727. Springer Nature Switzerland Cham, 2022. 1
- [16] Qing Jiang, Feng Li, Zhaoyang Zeng, Tianhe Ren, Shilong Liu, and Lei Zhang. T-rex2: Towards generic object detection via text-visual prompt synergy. In *European Conference on Computer Vision*, pages 38–57. Springer, 2024. 1, 2, 3
- [17] Lei Jin, Gen Luo, Yiyi Zhou, Xiaoshuai Sun, Guannan Jiang, Annan Shu, and Rongrong Ji. Refclip: A universal teacher for weakly supervised referring expression comprehension. In *Proceedings of the IEEE/CVF conference on computer vision and pattern recognition*, pages 2681–2690, 2023. 2
- [18] Aishwarya Kamath, Mannat Singh, Yann LeCun, Gabriel Synnaeve, Ishan Misra, and Nicolas Carion. Mdetrm: Modulated detection for end-to-end multi-modal understanding. In *Proceedings of the IEEE/CVF international conference on computer vision*, pages 1780–1790, 2021. 12
- [19] Sahar Kazemzadeh, Vicente Ordonez, Mark Matten, and Tamara Berg. Referitgame: Referring to objects in photographs of natural scenes. In *Proceedings of the 2014 conference on empirical methods in natural language processing (EMNLP)*, pages 787–798, 2014. 2, 5
- [20] Alexander Kirillov, Eric Mintun, Nikhila Ravi, Hanzi Mao, Chloe Rolland, Laura Gustafson, Tete Xiao, Spencer Whitehead, Alexander C Berg, Wan-Yen Lo, et al. Segment any-

- thing. In *Proceedings of the IEEE/CVF international conference on computer vision*, pages 4015–4026, 2023. 3
- [21] Xin Lai, Zhuotao Tian, Yukang Chen, Yanwei Li, Yuhui Yuan, Shu Liu, and Jiaya Jia. Lisa: Reasoning segmentation via large language model. In *Proceedings of the IEEE/CVF Conference on Computer Vision and Pattern Recognition*, pages 9579–9589, 2024. 2, 6, 7, 8
- [22] Feng Li, Qing Jiang, Hao Zhang, Tianhe Ren, Shilong Liu, Xueyan Zou, Huaizhe Xu, Hongyang Li, Jianwei Yang, Chunyuan Li, et al. Visual in-context prompting. In *Proceedings of the IEEE/CVF Conference on Computer Vision and Pattern Recognition*, pages 12861–12871, 2024. 1, 2, 3
- [23] Feng Li, Hao Zhang, Peize Sun, Xueyan Zou, Shilong Liu, Chunyuan Li, Jianwei Yang, Lei Zhang, and Jianfeng Gao. Segment and recognize anything at any granularity. In *European Conference on Computer Vision*, pages 467–484. Springer, 2024. 3
- [24] Ruiyu Li, Kaican Li, Yi-Chun Kuo, Michelle Shu, Xiaojuan Qi, Xiaoyong Shen, and Jiaya Jia. Referring image segmentation via recurrent refinement networks. In *Proceedings of the IEEE Conference on Computer Vision and Pattern Recognition*, pages 5745–5753, 2018. 3
- [25] Tsung-Yi Lin, Michael Maire, Serge Belongie, James Hays, Pietro Perona, Deva Ramanan, Piotr Dollár, and C Lawrence Zitnick. Microsoft coco: Common objects in context. In *Computer vision—ECCV 2014: 13th European conference, zurich, Switzerland, September 6–12, 2014, proceedings, part v 13*, pages 740–755. Springer International Publishing, 2014. 5
- [26] Chang Liu, Henghui Ding, and Xudong Jiang. Gres: Generalized referring expression segmentation. In *Proceedings of the IEEE/CVF conference on computer vision and pattern recognition*, pages 23592–23601, 2023. 1, 2, 3, 5, 6, 7, 12
- [27] Jiang Liu, Hui Ding, Zhaowei Cai, Yuting Zhang, Ravi Kumar Satzoda, Vijay Mahadevan, and R Manmatha. Polyformer: Referring image segmentation as sequential polygon generation. In *Proceedings of the IEEE/CVF conference on computer vision and pattern recognition*, pages 18653–18663, 2023. 2, 3
- [28] Shilong Liu, Zhaoyang Zeng, Tianhe Ren, Feng Li, Hao Zhang, Jie Yang, Qing Jiang, Chunyuan Li, Jianwei Yang, Hang Su, et al. Grounding dino: Marrying dino with grounded pre-training for open-set object detection. In *European Conference on Computer Vision*, pages 38–55. Springer, 2024. 2
- [29] Ting Liu and Siyuan Li. Hybrid global-local representation with augmented spatial guidance for zero-shot referring image segmentation. In *Proceedings of the Computer Vision and Pattern Recognition Conference*, pages 29634–29643, 2025. 2
- [30] Yang Liu, Muzhi Zhu, Hengtao Li, Hao Chen, Xinlong Wang, and Chunhua Shen. Matcher: Segment anything with one shot using all-purpose feature matching. *arXiv preprint arXiv:2305.13310*, 2023. 1, 3, 6
- [31] Ze Liu, Yutong Lin, Yue Cao, Han Hu, Yixuan Wei, Zheng Zhang, Stephen Lin, and Baining Guo. Swin transformer: Hierarchical vision transformer using shifted windows. In *Proceedings of the IEEE/CVF international conference on computer vision*, pages 10012–10022, 2021. 13
- [32] Ilya Loshchilov and Frank Hutter. Decoupled weight decay regularization. *arXiv preprint arXiv:1711.05101*, 2017. 13
- [33] Gen Luo, Yiyi Zhou, Xiaoshuai Sun, Liujuan Cao, Chenglin Wu, Cheng Deng, and Rongrong Ji. Multi-task collaborative network for joint referring expression comprehension and segmentation. In *Proceedings of the IEEE/CVF Conference on computer vision and pattern recognition*, pages 10034–10043, 2020. 1, 2
- [34] Zhuoyan Luo, Yinghao Wu, Tianheng Cheng, Yong Liu, Yicheng Xiao, Hongfa Wang, Xiao-Ping Zhang, and Yujiu Yang. Cohd: A counting-aware hierarchical decoding framework for generalized referring expression segmentation. In *Proceedings of the IEEE/CVF International Conference on Computer Vision*, pages 22685–22694, 2025. 2
- [35] Junhua Mao, Jonathan Huang, Alexander Toshev, Oana Camburu, Alan L Yuille, and Kevin Murphy. Generation and comprehension of unambiguous object descriptions. In *Proceedings of the IEEE conference on computer vision and pattern recognition*, pages 11–20, 2016. 2
- [36] Juhong Min, Dahyun Kang, and Minsu Cho. Hypercorrelation squeeze for few-shot segmentation. In *Proceedings of the IEEE/CVF international conference on computer vision*, pages 6941–6952, 2021. 3
- [37] Prashant Pandey, Mustafa Chasmai, Monish Natarajan, and Brejesh Lall. Weakly supervised few-shot and zero-shot semantic segmentation with mean instance aware prompt learning. In *2023 IEEE International Conference on Multimedia and Expo (ICME)*, pages 1–6. IEEE, 2023. 7, 8
- [38] Bohao Peng, Zhuotao Tian, Xiaoyang Wu, Chengyao Wang, Shu Liu, Jingyong Su, and Jiaya Jia. Hierarchical dense correlation distillation for few-shot segmentation. In *Proceedings of the IEEE/CVF Conference on Computer Vision and Pattern Recognition*, pages 23641–23651, 2023. 3
- [39] Shaoqing Ren, Kaiming He, Ross Girshick, and Jian Sun. Faster r-cnn: Towards real-time object detection with region proposal networks. *Advances in neural information processing systems*, 28, 2015. 1
- [40] Zhongwei Ren, Zhicheng Huang, Yunchao Wei, Yao Zhao, Dongmei Fu, Jiashi Feng, and Xiaoje Jin. Pixellm: Pixel reasoning with large multimodal model. In *Proceedings of the IEEE/CVF Conference on Computer Vision and Pattern Recognition*, pages 26374–26383, 2024. 7, 8
- [41] Nisarg A Shah, Vibashan VS, and Vishal M Patel. Lqm-former: Language-aware query mask transformer for referring image segmentation. In *Proceedings of the IEEE/CVF Conference on Computer Vision and Pattern Recognition*, pages 12903–12913, 2024. 7
- [42] Hengcan Shi, Hongliang Li, Fanman Meng, and Qingbo Wu. Key-word-aware network for referring expression image segmentation. In *Proceedings of the European Conference on Computer Vision (ECCV)*, pages 38–54, 2018. 3
- [43] Xinyu Shi, Dong Wei, Yu Zhang, Donghuan Lu, Munan Ning, Jiashun Chen, Kai Ma, and Yefeng Zheng. Dense cross-query-and-support attention weighted mask aggregation for few-shot segmentation. In *European Conference on Computer Vision*, pages 151–168. Springer, 2022. 6

- [44] Jiamu Sun, Gen Luo, Yiyi Zhou, Xiaoshuai Sun, Guan-nan Jiang, Zhiyu Wang, and Rongrong Ji. Refteacher: A strong baseline for semi-supervised referring expression comprehension. In *Proceedings of the IEEE/CVF conference on computer vision and pattern recognition*, pages 19144–19154, 2023. 2
- [45] Yanpeng Sun, Jiahui Chen, Shan Zhang, Xinyu Zhang, Qiang Chen, Gang Zhang, Errui Ding, Jingdong Wang, and Zechao Li. Vrp-sam: Sam with visual reference prompt. In *Proceedings of the IEEE/CVF Conference on Computer Vision and Pattern Recognition*, pages 23565–23574, 2024. 1, 3, 6
- [46] Wei Suo, Lanqing Lai, Mengyang Sun, Hanwang Zhang, Peng Wang, and Yanning Zhang. Rethinking and improving visual prompt selection for in-context learning segmentation. In *European Conference on Computer Vision*, pages 18–35. Springer, 2024. 1, 3
- [47] Zhuotao Tian, Hengshuang Zhao, Michelle Shu, Zhicheng Yang, Ruiyu Li, and Jiaya Jia. Prior guided feature enrichment network for few-shot segmentation. *IEEE transactions on pattern analysis and machine intelligence*, 44(2):1050–1065, 2020. 3
- [48] Wenxuan Wang, Tongtian Yue, Yisi Zhang, Longteng Guo, Xingjian He, Xinlong Wang, and Jing Liu. Unveiling parts beyond objects: Towards finer-granularity referring expression segmentation. In *Proceedings of the IEEE/CVF Conference on Computer Vision and Pattern Recognition*, pages 12998–13008, 2024. 2
- [49] Xinlong Wang, Wen Wang, Yue Cao, Chunhua Shen, and Tiejun Huang. Images speak in images: A generalist painter for in-context visual learning. In *Proceedings of the IEEE/CVF Conference on Computer Vision and Pattern Recognition*, pages 6830–6839, 2023. 7, 8
- [50] Zhaoqing Wang, Yu Lu, Qiang Li, Xunqiang Tao, Yandong Guo, Mingming Gong, and Tongliang Liu. Cris: Clip-driven referring image segmentation. In *Proceedings of the IEEE/CVF conference on computer vision and pattern recognition*, pages 11686–11695, 2022. 3
- [51] Zhuofan Xia, Dongchen Han, Yizeng Han, Xuran Pan, Shiji Song, and Gao Huang. Gsva: Generalized segmentation via multimodal large language models. In *Proceedings of the IEEE/CVF Conference on Computer Vision and Pattern Recognition*, pages 3858–3869, 2024. 2, 3, 6, 7
- [52] Linhui Xiao, Xiaoshan Yang, Xiangyuan Lan, Yaowei Wang, and Changsheng Xu. Towards visual grounding: A survey. *arXiv preprint arXiv:2412.20206*, 2024. 2
- [53] Qianxiong Xu, Lanyun Zhu, Xuanyi Liu, Guosheng Lin, Cheng Long, Ziyue Li, and Rui Zhao. Unlocking the power of sam 2 for few-shot segmentation. *arXiv preprint arXiv:2505.14100*, 2025. 1
- [54] Yuhuan Yang, Chaofan Ma, Jiangchao Yao, Zhun Zhong, Ya Zhang, and Yanfeng Wang. Remamber: Referring image segmentation with mamba twister. In *European Conference on Computer Vision*, pages 108–126. Springer, 2024. 2
- [55] Zhao Yang, Jiaqi Wang, Yansong Tang, Kai Chen, Hengshuang Zhao, and Philip HS Torr. Lavt: Language-aware vision transformer for referring image segmentation. In *Proceedings of the IEEE/CVF conference on computer vision and pattern recognition*, pages 18155–18165, 2022. 1, 7
- [56] Licheng Yu, Patrick Poirson, Shan Yang, Alexander C Berg, and Tamara L Berg. Modeling context in referring expressions. In *Computer Vision–ECCV 2016: 14th European Conference, Amsterdam, The Netherlands, October 11–14, 2016, Proceedings, Part II 14*, pages 69–85. Springer, 2016. 2, 5
- [57] Licheng Yu, Zhe Lin, Xiaohui Shen, Jimei Yang, Xin Lu, Mohit Bansal, and Tamara L Berg. Mattrnet: Modular attention network for referring expression comprehension. In *Proceedings of the IEEE conference on computer vision and pattern recognition*, pages 1307–1315, 2018. 3
- [58] Seonghoon Yu, Joonbeom Hong, Joonseok Lee, and Jeany Son. Latent expression generation for referring image segmentation and grounding. In *Proceedings of the IEEE/CVF International Conference on Computer Vision*, pages 21374–21383, 2025. 2
- [59] Anqi Zhang, Guangyu Gao, Jianbo Jiao, Chi Liu, and Yun-chao Wei. Bridge the points: Graph-based few-shot segment anything semantically. *Advances in Neural Information Processing Systems*, 37:33232–33261, 2024. 1, 3, 6
- [60] Renrui Zhang, Zhengkai Jiang, Ziyu Guo, Shilin Yan, Junting Pan, Xianzheng Ma, Hao Dong, Peng Gao, and Hongsheng Li. Personalize segment anything model with one shot. *arXiv preprint arXiv:2305.03048*, 2023. 3, 7, 8
- [61] Chaoyang Zhu, Yiyi Zhou, Yunhang Shen, Gen Luo, Xingjia Pan, Mingbao Lin, Chao Chen, Lijuan Cao, Xiaoshuai Sun, and Rongrong Ji. Seqtr: A simple yet universal network for visual grounding. In *European Conference on Computer Vision*, pages 598–615. Springer, 2022. 2
- [62] Xueyan Zou, Jianwei Yang, Hao Zhang, Feng Li, Linjie Li, Jianfeng Wang, Lijuan Wang, Jianfeng Gao, and Yong Jae Lee. Segment everything everywhere all at once. *Advances in neural information processing systems*, 36:19769–19782, 2023. 2, 3



In this appendix, we first provide additional details on the OmniSegNet method, including the Omni-Prompt Encoder for encoding visual prompts and the Mask Decoder for decoding the target mask. We then describe the model’s implementation, including the encoder architecture, parameter configuration, and training loss. For ablation experiments, the analyses of visual prompt types and *Prompt Embedding Module* (PEM) fusion strategies are presented in the main paper. This supplement reports the remaining ablation, focusing on the impact of the sampling ratio between text- and visual-guided data during training, further validating the significance of this design choice.

## A. Method

### A.1. Omni-Prompt Encoder

To handle the effective fusion of visual prompts, we propose a novel *omni-prompt encoder* for OmniSegNet, which consists of two modules, namely *Prompt Embed Module* (PEM) and *Prompt Generator*.

**Prompt Embed Module (PEM).** As shown in Fig. 8, the visual prompt is initially processed by the PEM to generate the visual prompt encoding. The PEM employs its internal convolution layer to map the input visual prompt into the same semantic space as the reference multi-scale visual features  $\mathbf{F}_r$ , achieving feature alignment. In each convolution layer  $\text{Conv}_i$ , the visual prompt  $\mathbf{P}^{(i)}$  is first passed through a convolutional transformation, and the resulting features are then element-wise added to the reference visual features at the corresponding scale, where  $i \in \{0, 1, 2, 3\}$ . This operation can be expressed as:

$$\mathbf{F}_s'^{(i)} = \mathbf{F}_r^i + \text{Conv}_i(\mathbf{P}^{(i)}), \quad (5)$$

Here,  $\mathbf{F}_s'^{(i)}$  represents the reference visual features at scale  $i$ . To further integrate multi-scale information, the set of scaled features  $\mathbf{F}_s'^{(i)}$  across different scales is flattened and concatenated along the channel dimension. This process yields a unified reference feature representation  $\mathbf{F}_r'$  that captures rich multi-scale context for subsequent processing stages.

**Prompt Generator.** The Prompt Generator extracts discriminative prompt features via a compact three-layer architecture, as illustrated in Fig. 8. Each layer consists of *deformable cross-attention* [18], *self-attention* and a *feed-forward network* (FFN). Given a set of learnable prompt queries  $\mathbf{F}_q \in \mathbb{R}^{n \times c}$ , where  $n$  denotes the number of queries and  $c$  is the feature dimension, the module first performs cross-attention with the reference features  $\mathbf{F}_r'$  from the PEM to capture essential object semantics:

$$\mathbf{F}_q' = \text{DeformCrossAttn}(\mathbf{F}_q, \mathbf{F}_r'), \quad (6)$$

The resulting query features  $\mathbf{F}_q'$  are then refined through self-attention to model global dependencies and passed

through an FFN for transformation:

$$\mathbf{F}_p = \text{FFN}(\text{SelfAttn}(\mathbf{F}_q')). \quad (7)$$

After three stacked layers of such processing, the final visual prompt features  $\mathbf{F}_p$  are obtained, which effectively encode semantic prompts from the reference and guide foreground segmentation in the target image.

### A.2. Mask Decoder

The Mask Decoder consists of three sequential blocks, each comprising two cross-attention layers, one self-attention layer and one FFN. The decoder takes as input: (1) a learnable segmentation query  $\mathbf{F}_{seg}$ , (2) a prompt feature  $\mathbf{F}_{pt}$  (either from the text or visual reference), and (3) multi-scale mask features  $\mathbf{F}_m^i$  from the target image, where  $i \in \{1, 2, 3\}$ . In each block  $i$ , the process is as follows:

$$\mathbf{F}_{seg} = \text{CrossAttn}(\mathbf{F}_{seg}, \mathbf{F}_m^i), \quad (8)$$

$$\mathbf{F}_{seg} = \text{CrossAttn}(\mathbf{F}_{seg}, \mathbf{F}_{pt}), \quad (9)$$

$$\mathbf{F}_{seg} = \text{FFN}(\text{SelfAttn}(\mathbf{F}_{seg})). \quad (10)$$

The updated  $\mathbf{F}_{seg}$  is propagated to the next block. After the third block, the final  $\mathbf{F}_{seg}$  is treated as the region feature  $\mathbf{F}_{reg}$ . This feature is fused with the low-level visual feature  $\mathbf{F}_m^0$  and passed to a MaskHead to produce the final segmentation mask. Additionally,  $\mathbf{F}_{reg}$  is processed by an MLP to generate the no-target prediction.

### A.3. Loss Setting

Our framework employs three training objectives for supervised optimization to enhance the segmentation performance. Drawing on the approach in [26], we introduce the cross-entropy loss as the basic loss function. Firstly, we define  $\mathcal{L}_{mask}$  to measure the difference between the ground truth label  $\mathbf{M}_{gt}$  and the final predicted mask  $\mathbf{M}_{pre}$ , ensuring that the model accurately identifies the target region. Secondly, we design  $\mathcal{L}_{region}$  to optimize the learning of the regional feature  $\mathbf{F}_{reg}$ . This loss measures the degree of matching between the regional feature  $\mathbf{F}_{reg}$  and the corresponding regional mask  $\mathbf{M}_{region}$ . Here,  $\mathbf{M}_{region}$  is adjusted to the same scale as  $\mathbf{F}_{reg}$  by performing linear interpolation on the ground truth mask  $\mathbf{M}_{gt}$ . Additionally, to further improve the model’s ability to detect the presence of the target, we apply global average pooling to all regional features  $\mathbf{F}_{reg}$  and predict the target’s existence  $\mathbf{P}_{gt}$  based on the pooling results  $\mathbf{P}_{pre}$ . To this end, we introduce the  $\mathcal{L}_{nt}$  loss function, which optimizes the accuracy of the target existence prediction. Therefore, the total loss with balance factor  $\lambda$  is:

$$\mathcal{L}_{total} = \lambda_1 \mathcal{L}_{mask} + \lambda_2 \mathcal{L}_{region} + \lambda_3 \mathcal{L}_{nt}. \quad (11)$$

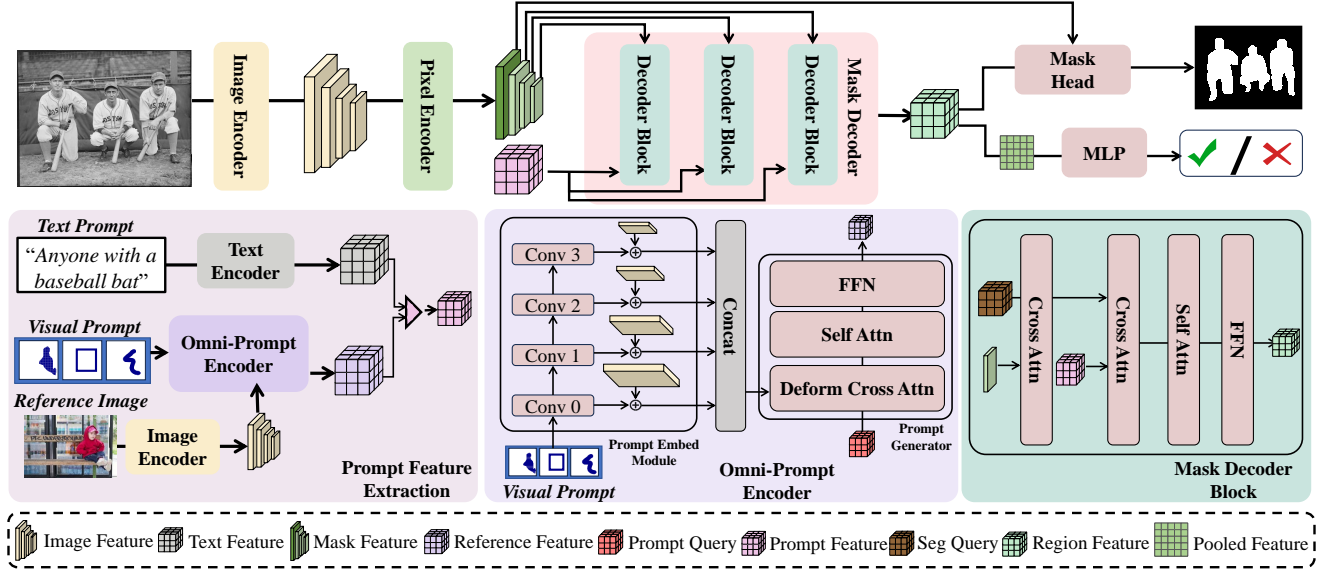


Figure 8. The architecture of the proposed baseline model, termed OmniSegNet. The target image is processed by the image encoder and the pixel encoder to obtain multi-scale visual features for accurate mask decoding. When input text prompts only, the text features extracted by the text encoder will be directly fed to the mask decoder for cross-modal interaction. OmniSegNet also introduces a novel omni-prompt encoder to handle the spatial prompts, such as masks, boxes and scribbles. With this omni-prompt encoder, the semantics of the visual referent in the image can be extracted to guide mask decoding. OmniSegNet can also support the processing of visual and text prompts at the same time.

## B. More Experiments

### B.1. Implementation Settings

We adopt the Omni-Prompt Encoder as our core architecture. We employ three sets of deformable cross-attention, self-attention and FFN modules within its Prompt Generator, each with a feature dimension of 256. To ensure alignment between text and visual prompt features, the length of Prompt Query is set to the predefined maximum sentence length, enabling both modalities to share the same Mask Decoder. The Mask Decoder is composed of nine mask decoder blocks, grouped into three groups, each corresponding to one scale of features extracted by the Pixel Encoder. We use Swin-B [31] as the image encoder and BERT [4] as the text encoder with a hidden dimension of 768. During training, the input images are resized to  $480 \times 480$  and the maximum sentence length is fixed at 20. The model is optimized using AdamW [32] with a weight decay of 0.05. The initial learning rate is set to  $1e-5$  and follows a polynomial decay schedule.

### B.2. Ablation Study of OmniSegNet

**Effect of Batch Sample Ratio.** Tab. 5 presents a comparative analysis of using different batch sample ratios during joint training of the gRefCOCO dataset and visual prompt data from the OmniRef benchmark. The evaluation datasets are their respective test sets, and the impact of varying ratios

Table 5. Ablation study of the batch sample ratios in our training regimes.

Ratio	gRefCOCO-val			Visual-test		
	cIoU	gIoU	N <sub>acc</sub>	cIoU	gIoU	N <sub>acc</sub>
-	64.21	65.53	58.72	75.35	66.36	89.48
5/3	63.98	65.36	59.37	76.34	67.61	90.12
9/4	64.50	66.00	59.78	76.29	67.79	89.86
7/3	64.22	65.61	57.64	76.39	68.12	89.77
5/2	64.10	66.49	61.48	76.51	68.30	90.23
3/1	64.75	66.81	61.43	76.51	68.22	89.91
7/2	<b>65.30</b>	<b>67.57</b>	<b>63.44</b>	<b>76.63</b>	<b>68.87</b>	<b>90.81</b>

on gRefCOCO-val and Visual-test performance is assessed. Notably, the first row (“-”) reports the results of training the model independently on each dataset—gRefCOCO for text-guided referring segmentation, and OmniRef visual prompt data for visual-guided segmentation. These results provide a baseline for understanding how much joint training contributes beyond single-modality supervision. For gRefCOCO-val, increasing the proportion of text-guided samples significantly improves performance, indicating that rich language supervision helps the model better understand and express natural language referring cues. Compared with the “-” baseline, nearly all mixed ratios produce higher cIoU, gIoU, and N<sub>acc</sub>, demonstrating that incorpo-

rating visual-guided samples does not harm text-guided performance and can even improve generalization. On Visual-test, adding more visual-guided samples improves performance, but the gains remain relatively stable across different ratios. However, joint training consistently outperforms the standalone (“-”) baseline, suggesting that text-guided signals also provide auxiliary benefits for visual prompt understanding. In summary, the 7/2 ratio achieves the best performance in both tasks, balancing text and visual prompt learning. These observations demonstrate that joint training is not a simple combination of two tasks; instead, it enables beneficial cross-modality transfer, effectively surpassing the standalone (“-”) baselines and confirming the value of strategic data distribution in multimodal segmentation training.